ICRIE 2023 4th INTERNATIONAL CONFERENCE ON RECENT INNOVATIONS IN ENGINEERING

Proceedings of the 4th International Conference on Recent Innovation in Engineering
ICRIE 2023, University of Duhok, College of Engineering, 13th – 14th September 2023
(Special issue for Passer journal of basic and applied sciences)
Paper No. 22

RESEMBLING THE MORPHOLOGIES OF ECG SIGNALS USING REGULARIZED DENOISING AUTOENCODER

Fars Samann[1,2]*, and Thomas Schanze[1]
1 Institute for Biomedical Engineering, Faculty of Life Science Engineering (LSE), Technische Hochschule Mittelhessen (THM) - University of Applied Sciences, Germany
2 Department of Biomedical Engineering, College of Engineering, University of Duhok, Kurdistan Region, Iraq
* Corresponding author: Institute for Biomedical Engineering, Faculty of Life Science Engineering (LSE), Technische Hochschule Mittelhessen (THM) - University of Applied Sciences, Germany. Tel: +491774006256.
thomas.schanze@lse.thm.de; fars.samann@uod.ac

ABSTRACT

ECG recording often requires an effective method of denoising to provide a clean signal for an accurate and valid diagnosis. Denoising autoencoder (DAE) has shown optimistic results in denoising ECG signals, especially a simple DAE consisting of input, hidden, and output layers. However, to obtain a good and efficient denoising, the optimal number of hidden neurons needs to be estimated. If the number of neurons in the hidden layer is less than those of the input or output layer, a dimension reduction occurs, which is known as the 'bottleneck effect'. This forces the DAE network to learn the relevant feature map of the input during training. Here, we propose a framework to denoise the ECG segments using a regularized denoising autoencoder (RDAE), with one hidden layer only, where the bottleneck effect is introduced by applying a sparsity penalty or regularizations to the weights to learn sparse feature maps instead of the redundant information in the input signals. In this work, $\boldsymbol{L_1}$ and $\boldsymbol{L_2}$ Kernel regularizations are evaluated in terms of denoising ECG signals. The optimal regularization parameter is evaluated using a statistical method known as the Gini index, to find the optimal trained decoding weights which resemble the morphologies of the ECG signal efficiently. In conclusion, the $\boldsymbol{L_1}$- and $\boldsymbol{L_2}$ -RDAE models with a suitable regularization parameter can effectively capture features that resemble the morphologies of ECG signals from its noisy version with an average signal-to-noise ratio improvement of 13.60 dB and 10 dB, respectively.

KEYWORDS: Regularized denoising autoencoder; Kernel regularization; Resembling signal; Denoising ECG signals.

1 INTRODUCTION

Electrocardiogram, known as ECG, is a non-invasive test to diagnose cardiovascular disease (CVD) and to assess the condition of the heart. To check the abnormality of the heart, an ambulatory ECG monitoring test is often considered to detect/indicate abnormal cardio functions during long hours of recording ordinary daily activities. However, such ECG signals are often corrupted by different types of noises, like muscle/motion artefact, electrode movement, baseline wander, and Gaussian white noise. Therefore, several denoising methods have been proposed in the literature, such as discrete wavelet and

Savitzky-Golay filtering (Awal, Mostafa, & Ahmad, 2011), empirical mode decomposition (Kong, et al., 2018; Nguyen & Kim, 2016) and adaptive filtering (Joshi , Verma , & Singh , 2015). However, denoising of a noisy ECG signal should be done carefully with as few changes in the morphology of ECG signals. The current state-of-art in signal denoising is the use of neural network models such as denoising autoencoder (DAE) (Samann, & Schanze, 2021; Chiang, et al., 2019; Zezario, et al., 2020), which have a great performance in denoising complex bio-signals, for example, ECG signal (Samann, & Schanze, 2023).

In the last couple of years, several DAE models have been proposed in the literature to denoise bio-signals, such as ECG signals. These models encode the noisy training segments to lower dimensional representation to capture relevant feature maps. They often have a symmetric architecture with single or multiple hidden layers, using either fully connected layers (also known as dense layers) or convolutional layers. In contrast, the number of hidden neurons needs to be less than those at the input/output layer to enable dimensional reduction, which is known as the 'bottleneck effect'. Recently, fully convolutional network (FCN) and convolutional neural network (CNN) models have been used widely to denoised ECG signals through considering long input segment as proposed in (Chiang, et al., 2019; Qiu, et al., 2020; Wang, Liu, Peng, & Tsao, 2023). These deep learning models, which were previously addressed, share the usage of a long input signal and several hidden layers. We think that the sequential ECG epoch correlation in a lengthy input signal was used to improve the learning of these DAE models and subsequently denoising performance. The current DAE models, however, have the disadvantage of adopting excessively deep architectures with several hidden layers; as a result, the number of hidden neurons should be carefully estimated to provide effective denoising performance. In (Samann & Schanze, 2021; Samann & Schanze, 2023), Akaike's information criterion was used to determine the optimal number of hidden neurons that are necessary to denoise ECG segments in case of different noise types. Despite of the computational costs of estimating the number of hidden neurons, it is not practical in real-world applications to reset the hyperparameters with respect to noise type (Teoh , Tan , & Xiang , 2006). Here, we propose a method to denoise the ECG segments using a regularized denoising autoencoder (RDAE), with one hidden layer only, where the bottleneck effect is introduced by applying a sparsity penalty or regularizations to the weights to learn sparse feature maps instead of the redundant information in the input signals. In addition, L_1 and L_2 kernel regularizations are evaluated in terms of denoising ECG signals and resembling the morphologies of ECG signals efficiently. The optimal regularization parameter is evaluated using a statistical method known as Gini index to find the optimal trained decoding weights (Schubert & Schanze, 2019).

2 METHODOLOGY

The block diagram of the proposed denoising framework is demonstrated in Fig. 1.

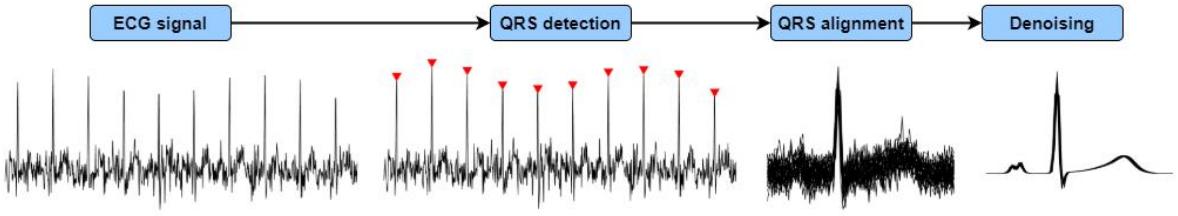

Figure 1: Block diagram of the proposed denoising framework.

2.1 Denoising Autoencoder (DAE)

The simple autoencoder (AE) encodes high dimensional data into lower dimensional data by considering one hidden layer with a smaller number of hidden neurons than those at the input/output layer (see Fig. 2A). This is known as the 'bottleneck effect' which forces the network to learn the relevant features

of the input during training, i.e., constructing relevant feature mappings. To capture a good feature map, the number of hidden neurons needs to be estimated (Samann & Schanze, 2021). In this work, the number of neurons at the input/output is denoted as N, and the number of hidden neurons at the hidden layer is denoted as K. The general assumption which makes the AE able to learn relevant features from the training dataset is $K < N$.

The denoising autoencoder is often trained with a noisy input signal. $\tilde{\mathbf{x}} \in \mathbb{R}^{N\times 1}$ to capture important features of the target signal $\mathbf{x} \in \mathbb{R}^{N\times 1}$ through dimension reduction, where the noisy input signal $\tilde{\mathbf{x}}$ is encoded into a latent representation $\mathbf{h} \in \mathbb{R}^{K\times 1}$, then decoded back to the denoised signal $\mathbf{y} \in \mathbb{R}^{N\times 1}$. Mathematically, it can be expressed as follows (Samann & Schanze, 2021),

$$\mathbf{h} = \mathbf{f}(\mathbf{W}\tilde{\mathbf{x}} + \mathbf{b}), \quad (1)$$

$$\mathbf{y} = \left(\hat{\mathbf{W}}\mathbf{h} + \hat{\mathbf{b}}\right), \quad (2)$$

where the pairs $\mathbf{W} \in \mathbb{R}^{K\times N}, \mathbf{b} \in \mathbb{R}^{K\times 1}$ and $\hat{\mathbf{W}} \in \mathbb{R}^{N\times K}, \hat{\mathbf{b}} \in \mathbb{R}^{N\times 1}$ are the encoding and decoding weights and biases, respectively. In this work, the hyperbolic tangent was chosen as the activation function $\mathbf{f}$. These weights and biases are updated in a backpropagation fashion to minimize the total error between the target signal $\mathbf{x}$ and the denoised signal $\mathbf{y}$. The common loss functions L for regression models (without constraining or regularization) are L_1-norm (denoted as mean absolute error) (Samann, Meyer, & Schanze, 2023),

$$L_1 = \frac{1}{N}\sum_{i=1}^{N}|\mathbf{x}_i - \mathbf{y}_i|, \quad (3)$$

and L_2-norm (known as mean square error), given as,

$$L_2 = \frac{1}{N}\sum_{i=1}^{N}(\mathbf{x}_i - \mathbf{y}_i)^2. \quad (4)$$

2.2 Regularized Denoising Autoencoder (RDAE)

The regularized denoising autoencoder is a denoising autoencoder model which often imposes a sparsity penalty or regularizations to the activations or the weights of the hidden layers to learn sparse feature maps instead of the redundant information in the input signals (Samann, Meyer, & Schanze, 2023). In the case of RDAE model, the number of hidden neurons at the hidden layer is typically equal to or larger than those at the input or output layer (either $K = N$ as in Fig. 3B or $K > N$ as in Fig. 3C). Besides, another term is included in the loss function to regularize the weights or activations of hidden neurons. Eq. 3 and 4 can be rewritten in case of L_1 and L_2 with corresponding regularizations of the weights (Samann, Meyer, & Schanze, 2023),

$$\text{Loss}_1 = L_1 + \lambda\sum_{i=1}^{N}|w_i|, \quad (5)$$

$$\text{Loss}_2 = L_2 + \lambda\sum_{i=1}^{N}w_i^2, \quad (6)$$

where λ is the regularization parameter. Weight regularization is commonly applied to both the encoder and decoder of RDAE model. The encoder and decoder weights of the proposed RDAE model have been subjected to the same regularization parameter λ.

Python 3.8 and the TensorFlow library were used to develop the proposed RDAE models. Adaptive moment estimation (with $\epsilon = 0.01, \alpha = 0.9$) was used as an optimizer with Eq. 5 and Eq. 6 as loss functions, respectively. Also, the 'EarlyStopping' algorithm (with epochs=200 and patience=20) was used to avoid overfitting.

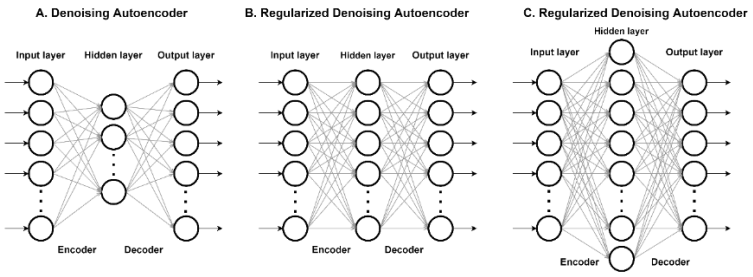

Figure 2. The feature map could be obtained by imposing 'bottleneck effect' at the hidden layer, as shown in A. Denoising autoencoder with the number of hidden neurons $K < N$, or by imposing weight or activation regularization to the hidden layer as shown in regularized denoising autoencoder model with number of hidden neurons B. $K = N$. C. $K > N$. Note: N is the number of neurons at the input/output layer.

2.3 Data preparation

A model for simulating ECG signals from PhysioNet is used to generate 50 ECG recordings of 98 beats each (Sološenko, et al., 2021). These ECG signals are segmented into 4,900 QRS-aligned segments of 98 segments per recording to create a ground truth dataset. Each segment has a length of 80 samples and a sampling frequency of 100 Hz. These aligned segments are divided into 2,940, 980, and 980 segments as training, validation, and testing datasets. To evaluate the denoising performance of RDAE, these ECG segments are superimposed with three recorded physical noises, which are obtained from (Moody, Muldrow , & Mark, 1984), namely, muscle/motion artifact (MA), electrode movement (EM), and baseline wander (BW), and simulated noise such as a Gaussian white noise (GWN). Four noise levels for each noise type are considered 10%, 30%, 50% and 80% $\sigma(x)$, where $\sigma(x)$ is the standard deviation of the ECG segment. For the training phase, all noise levels in addition to the clean ECG segments, were used to train the proposed RDAE model.

3. RESULTS AND DISCUSSIONS

In this work, different evaluation metrics are used to assess the performance of RDAE model, such as signal-to-noise ratio improvement (SNR_{imp}), percentage root-mean-square difference ($PRD\%$) and mean square error (MSE), respectively, as follows (Samann, & Schanze, 2021),

$$SNR_{imp}\,[dB] = 10\log_{10}\left(\frac{\sum_{n=1}^{N}|\,\tilde{\mathbf{x}}[n]-\mathbf{x}[n]|^2}{\sum_{n=1}^{N}|\mathbf{y}[n]-\mathbf{x}[n]|^2}\right), \tag{7}$$

$$PRD\% = \sqrt{\frac{\sum_{n=1}^{N}(\mathbf{x}[n]-\mathbf{y}[n])^2}{\sum_{n=1}^{N}(\mathbf{x}[n])^2}} \times 100, \tag{8}$$

$$MSE = \frac{1}{N}\sum_{n=1}^{N}(\mathbf{x}[n]-\mathbf{y}[n])^2. \tag{9}$$

where $\mathbf{x}[n]$, $\tilde{\mathbf{x}}[n]$ and $\mathbf{y}[n]$ are the original, noisy and denoised ECG segment, respectively. The performance of both L_1- and L_2- RDAE models for different values of λ are presented in table 1 and 2 respectively.

By training the RDAE model with QRS-aligned ECG segments, it has been found that the values of decoding weights for each hidden neuron have a direct relationship to the timestamp/features of the input segments. Based on this finding, the Gini index is considered to evaluate the sparsity of the trained decoding weights matrix, i.e., $\widehat{\mathbf{W}} \in \mathbb{R}^{N\times K}$ of K hidden neurons and N weights. In general, the Gini index is a statistical approach commonly used in economics to measure the inequality in income levels or wealth values. The Gini index of 0 denotes perfect equality or non-sparse, while Gini index of 1 denotes perfect inequality or sparsity (Dixon, Weiner, & Mitchell-Old, 1987). The Gini index for each decoding weight over the total hidden neurons could indicate how well the RDAE/ DAE models represent the morphologies

of the input segment. We calculate Gini index for the rth decoding weight over the total number of hidden neurons K as follow (Schubert, & Schanze, 2019),

$$G_r = \frac{\sum_{i=1}^{K}\sum_{j=1}^{K}|\widehat{w}_{r,i}-\widehat{w}_{r,j}|}{2N^2\bar{W}}, \text{ where } r = 1, 2, \dots, N. \quad (10)$$

It is worth mentioning that the optimal number of hidden neurons depends on the complexity of the data and the type of noise. It was proven by (Samann & Schanze, 2023) that noises, e.g., GWN, of completely overlapping power spectrum with the target signal require a small number of neurons compared with slightly overlapping power spectrum noises, e.g., BW (see Fig. 3). In other words, a large number of hidden neurons allows the RDAE model to learn a complex representation of the training data. As a rule of thumb, the minimum number of hidden neurons for both RDAE and DAE models is half of the input/output length, $K = N/2$. However, this could vary depending on the complexity of the task handled by the RDAE model. As a result, the ideal number of hidden neurons in this study was specified to be equal to the number of neurons in the input/output layer, $K = N$. Despite the fact that the DAE model achieved good results in denoising ECG signals (see Fig. 3), the RDAE model with a suitable regularization parameter λ captures more relevant features that resemble the morphologies of ECG signals (see Fig. 6 &7).

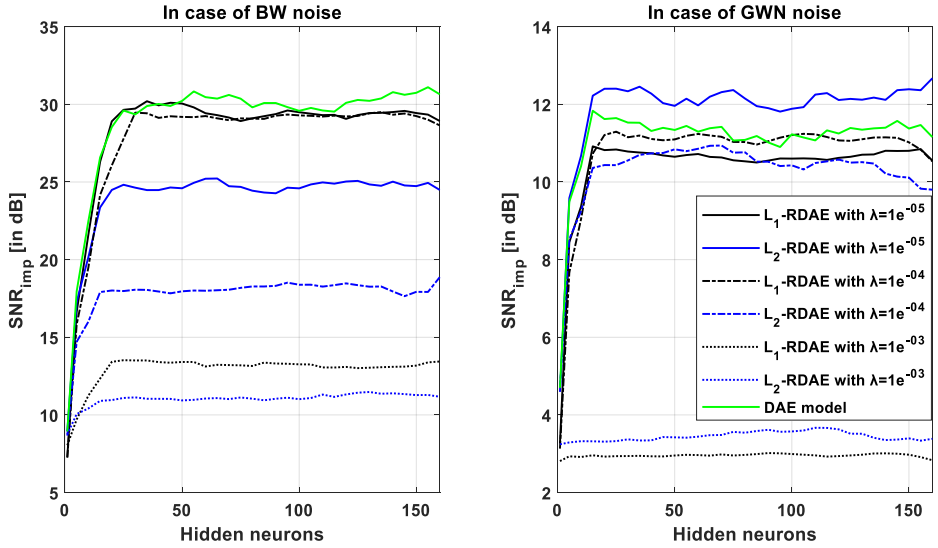

Figure 3: Plotting the SNR_{imp} of L_1- and L_2-RDAE model for different values of regularization parameter λ in case of (left) BW noise, (right) GWN noise with noise level=80%. The green curve represents the performance of DAE model (Samann & Schanze, 2023). Note that the range of the two plots is not similar.

Fig. 5, 6 and 7 show the effect of L_1 and L_2 weight regularization on the decoding weights of the RDAE model in the case of $\lambda = 1e^{-3}, 1e^{-4}$ and $1e^{-5}$, respectively. The timestamp of ECG morphologies like the P-wave, QRS complex, and T-wave mostly exhibit large Gini index values or high sparsity in the decoding weights of the L_1-RDAE model, especially in the cases of $\lambda = 1e^{-4}$ and $1e^{-5}$. On the other hand, the decoding weights of L_2-RDAE model revealed redundant ECG features, leading to low Gini index values. The smallest λ yields highly sparse decoding weights in the case of the L_1-RDAE model and better representation of ECG morphologies. However, as shown in Fig. 4, the decoding weights of the traditional DAE model do not resemble the primary characteristics of the ECG signal.

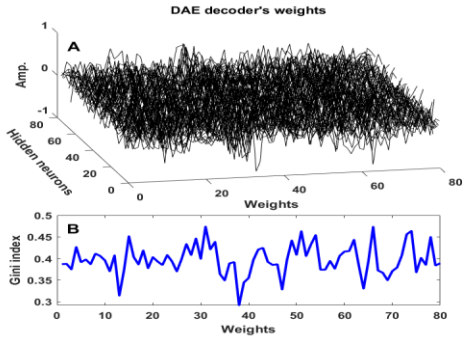

Figure 4: In the case of MA noise, the decoder's weights of the unregularized DAE model are plotted in A, and the Gini index values of these weights are calculated below in B. The low sparsity in the Gini index curve indicates that there is no link between the decoding weights and the morphologies of the ECG signal.

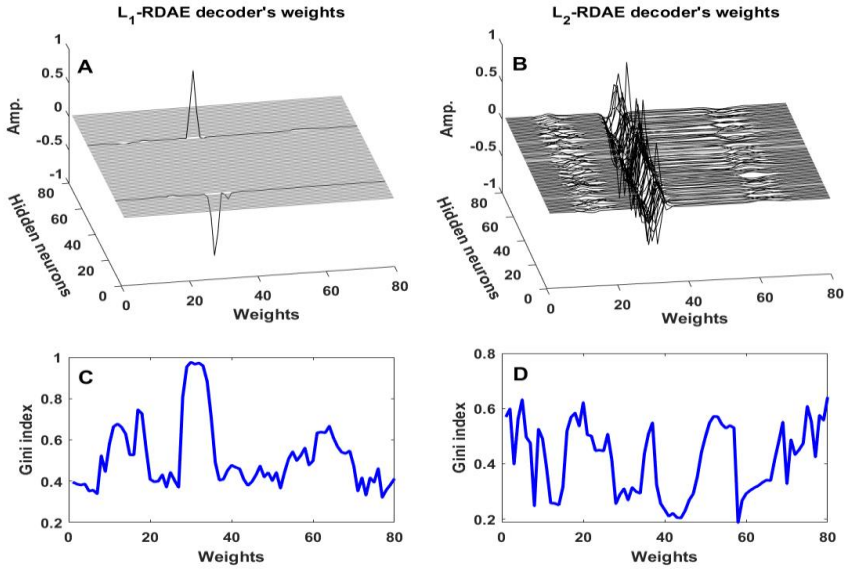

Figure 5: In the case of MA with $\lambda = 1e^{-3}$, the decoding weights are plotted for A. L_1-RDAE model and B. L_2-RDAE model and the Gini index values of these weights are calculated below each case in C. and D., respectively. Note: the hidden neurons with nonzero and zero weights are plotted in black and grey line, respectively. The Gini index curve for the L_1-RDAE model shows a high sparsity, especially at the weights linked to the timestamp of QRS-complex, while the L_2-RDAE model exhibits low sparsity due to the redundant representation of ECG's morphologies, e.g., P-wave, QRS-complex and T-wave.

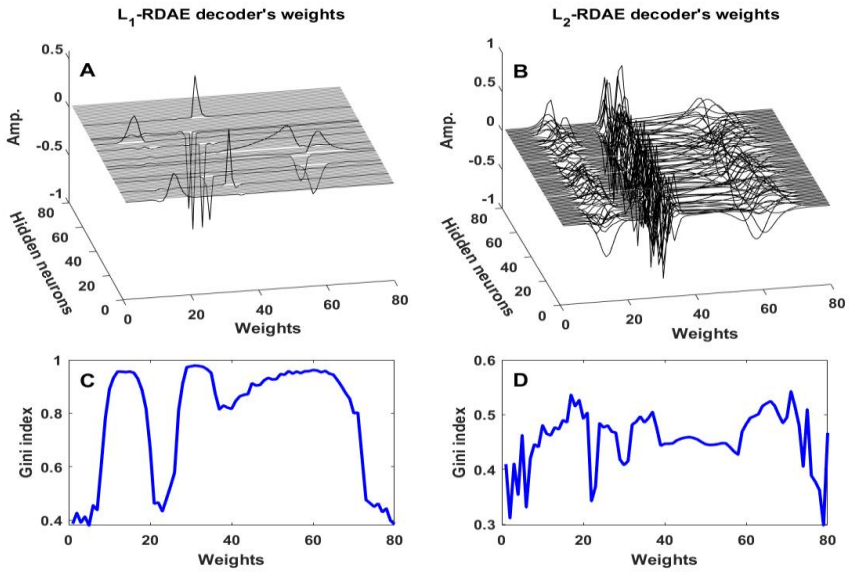

Figure 6: In case of MA noise with $\lambda = 1e^{-}$, the decoding weights are plotted for A. L_1-RDAE model and B. L_2-RDAE model, and the Gini index values of these weights are calculated below each case in C. and D., respectively. Note: the hidden neurons with nonzero and zero weights are plotted in black and gray line, respectively. The Gini index curve for the L_1-RDAE model shows a high sparsity at the weights linked to the timestamp of P-wave, QRS-complex and T-wave, while the L_2-RDAE model exhibits low sparsity due to the redundant representation of ECG's morphologies.

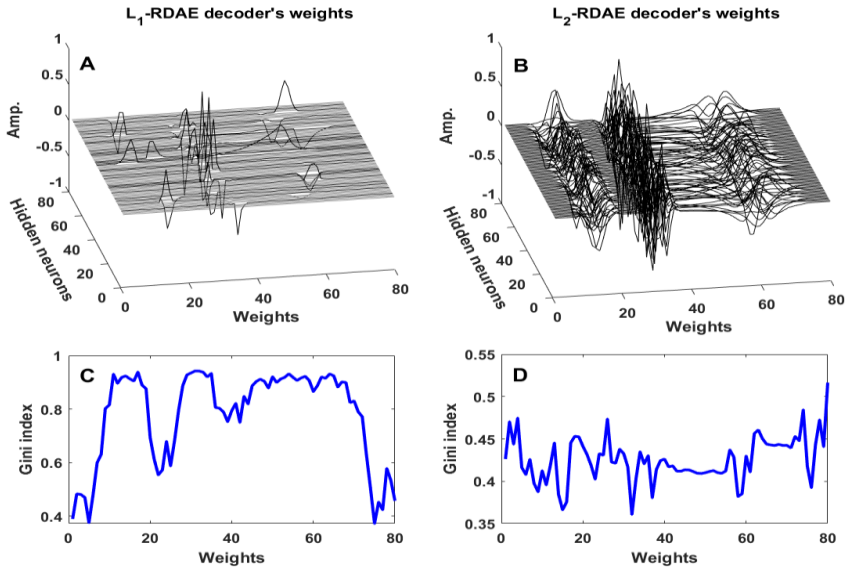

Figure 7: In case of MA noise with $\lambda = 1e^{-5}$, the decoding weights are plotted for A. L_1-RDAE model and B. L_2-RDAE model, and the Gini index values of these weights are calculated below each case in C. and D., respectively. Note: the hidden neurons with nonzero and zero weights are plotted in black and gray line, respectively. The Gini index curve for the L_1-RDAE model shows a high sparsity at the weights linked to the timestamp of P-wave, QRS-complex and T-wave, while the L_2-RDAE model exhibits low sparsity due to the redundant representation of ECG's morphologies.

In Fig. 8 & 9, we demonstrated the decoding weights, which correspond to large hidden neurons, and how closely they resemble the denoised ECG segment. It is clearly detectable/apparent that few decoding

weights in case of L_1-RDAE model are sufficient to reconstruct the original ECG segment with few numbers of large hidden neurons compared to L_2-RDAE model. Besides, in case of L_1-RDAE model, plenty of the hidden neurons are near to zero or exactly zero compared to L_2-RDAE model as shown clearly in Fig. 8 and 9.

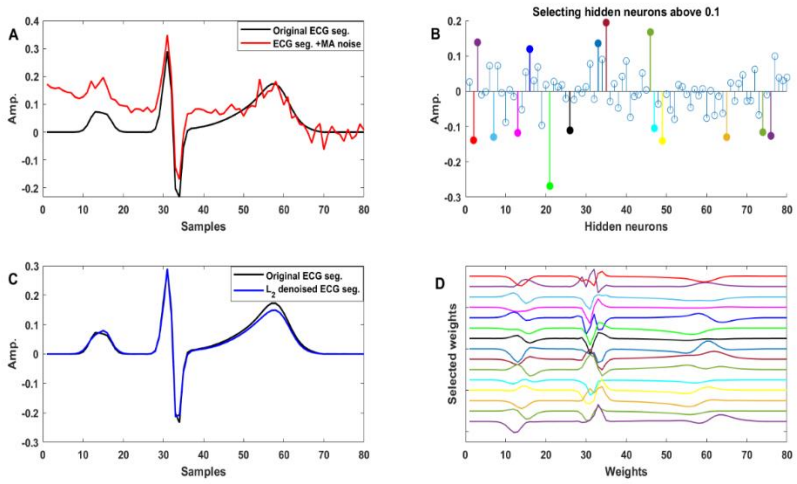

Figure 8: B. Showing the activation value of hidden neurons after applying a noisy ECG segment from the testing dataset, which is corrupted with MA of noise level= 80%, to the L_2-RDAE model. D. Displaying the corresponding weights of the selected hidden neurons, which have activation value above 0.1. L_2-RDAE model enforces dimension reduction or 'bottleneck effect' by making few neurons to be large only as shown in B. and D.

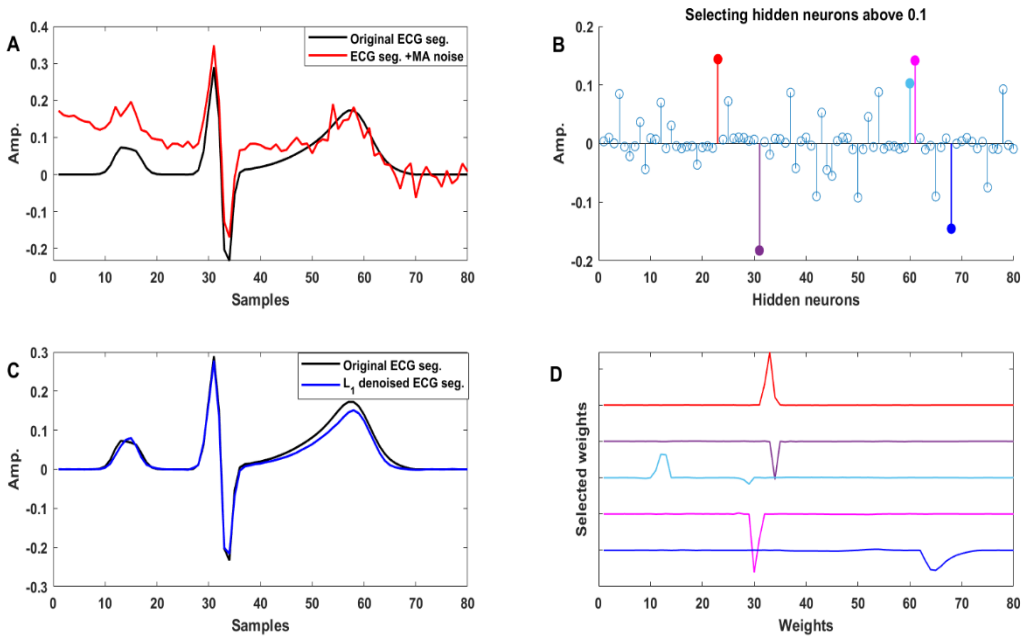

Figure 9. B. Showing the activation value of hidden neurons after applying a noisy ECG segment from the testing dataset, which is corrupted with MA of noise level= 80%, to the L_1-RDAE model. D. Displaying the corresponding weights of the selected hidden neurons, which have activation value above

0.1. The resembling of ECG is clearly demonstrated in case of L_1-RDAE model due to the sparsity of decoder's weights. L_1-RDAE model enforces dimension reduction or 'bottleneck effect' by making few neurons to be large only as shown in B. and D.

Tables 1 shows that both L_1- and L_2-RDAE model performed inadequately with a value of $\lambda = 1e^{-3}$, especially in the case of low noise levels, while they performed significantly well with a value of $\lambda = 1e^{-5}$. Nevertheless, the L_1-RDAE model outperforms the L_2-RDAE model with average signal-to-noise ratio improvement of 3.60 dB for $\lambda = 1e^{-5}$ in case of low noise level= 10% and 30%. However, they performed approximately the same for high noise level=50% and 80%. This means that the highly sparse weights of L_1-RDAE model could adequately resemble the individual morphologies of ECG segment from its noisy version compared to the redundant weights of L_2-RDAE model as demonstrated in Fig. 6 & 7.

Table 1. The performance of L_1-RDAE model in denoising ECG from different types and levels of noise for $\lambda = 1e-3, 1e-4$ and $1e-5$.

Table 1: The performance of L_2-RDAE model in denoising ECG from different types and levels of noise for $\lambda = 1e-3, 1e-4$ and $1e-5$.

$L_2 - RDAE$		$\lambda = 1e-3$			$\lambda = 1e-4$			$\lambda = 1e-5$		
Noise type	**Noise level**	SNR_{imp} [dB]	$PRD\%$	MSE	SNR_{imp} [dB]	$PRD\%$	MSE	SNR_{imp} [dB]	$PRD\%$	MSE
MA	10 %	-12.08	6.10	9.70 e-04	-4.60	2.63	1.73 e-04	2.385	1.12	3.20e-05
	30 %	-2.55	6.10	9.72 e-04	4.67	2.69	1.82 e-04	10.83	1.28	4.30e-05
	50 %	1.86	6.12	9.75 e-04	8.70	2.82	2.01 e-04	13.95	1.53	6.53e-05
	80 %	5.90	6.14	9.83 e-04	12.05	3.08	2.44 e-04	16.19	1.97	1.15 e-04
EM	10 %	-10.05	6.19	9.95 e-04	-4.02	3.14	2.51 e-04	-0.13	1.97	1.03 e-04
	30 %	-0.55	6.22	10.21 e-04	5.12	3.28	2.85 e-04	8.54	2.19	1.36 e-04
	50 %	3.79	6.28	10.34 e-04	8.96	3.53	3.32 e-04	11.75	2.55	1.91 e-04
	80 %	7.69	6.41	10.71 e-04	11.99	4.01	4.65 e-04	13.93	3.22	3.15 e-04
BW	10 %	-14.37	6.12	9.64 e-04	-6.79	2.60	1.72 e-04	2.68	0.84	1.84 e-05
	30 %	-4.83	6.12	9.66 e-04	2.68	2.62	1.74 e-04	12.01	0.86	1.97 e-05
	50 %	-0.40	6.13	9.72 e-04	7.01	2.65	1.77 e-04	16.11	0.90	2.24e-05
	80 %	3.65	6.14	9.76 e-04	10.86	2.72	1.93 e-04	19.58	0.98	2.88 e-05
GWN	10 %	-8.62	6.17	9.81 e-04	-2.38	3.04	2.32 e-04	0.73	2.08	1.12 e-04
	30 %	0.89	6.20	9.91 e-04	6.42	3.29	2.74 e-04	8.46	2.55	1.64 e-04
	50 %	5.26	6.20	10.14 e-04	9.87	3.64	3.34 e-04	10.91	3.18	2.63 e-04
	80 %	9.17	6.34	10.41 e-04	12.11	4.50	5.26 e-04	12.11	4.47	5.24 e-04

4. CONCLUSION

A regularized denoising autoencoder model was proposed in this work to capture relevant features that resemble the morphologies of QRS-aligned ECG segments. Compared to the classical DAE model, the RDAE model imposes the dimensional reduction through applying a sparsity penalty or regularizations to

the weights to learn sparse feature maps instead of the redundant information in the input signals (Samann, Meyer & Schanze, 2023). In this work, L_1 and L_2 weight regularization were evaluated in denoising noisy ECG segments. The results clearly show that the RDAE model with a suitable regularization of weights can effectively capture features that resemble the morphologies of ECG signals from its noisy version. Moreover, L_1-RDAE model could resemble the morphologies of ECG signals more efficiently with few large hidden neurons compared to L_2-RDAE model. In other words, the L_1-RDAE model optimize the sparse and effective representation of ECG segments, where the weights of each hidden neuron capture a specific feature of the ECG segments, such as P-wave, QRS-complex, and T-wave. These captured features could also be used to compress the data by representing the morphologies of the wanted signal with the activity of a few numbers of hidden neurons. Thus, RDAE can be used to find a base for effective representation of signal components.

5. ACKNOWLEDGEMENTS

We would like to thank Deutscher Akademischer Austauschdienst (DAAD) organization for supporting the PhD work of Fars Samann (Grant Reference: 57507871).

REFERENCES

1. Awal, M., Mostafa, S., & Ahmad, M. (2011). Performance analysis of Savitzky-Golay smoothing filter using ECG signal. International Journal of Computer and Information Technology (IJCIT), 1(2), 24-29.
2. Chiang , H., Hsieh, Y., Fu , S., Hung , K., Tsao , Y., & Chien, S. (2019). Noise reduction in ECG signals using fully convolutional denoising autoencoders. IEEE Access, 7, 60806–60813. https://10.1109/ACCESS.2019.2912036.
3. Dixon, P., Weiner, J., & Mitchell-Old, T. (1987). Bootstrapping the Gini coefficient of Inequality. Ecology, 68(5), 1548-1551.
4. Joshi , V., Verma , A., & Singh , Y. (2015). Denoising of ECG signal using adaptive filter based on MPSO. Procedia Computer Science, 57, 395–402.
5. Kong, Q., Song , Q., Hai , Y., Gong , R., Liu , J., & Shao, X. (2018). Denoising signals for photoacoustic imaging in frequency domain based on empirical mode decomposition. Optik, 160, 402–14.
6. Moody, G., Muldrow , W., & Mark, R. (1984). A noise stress test for arrhythmia detectors. Computers in Cardiology, 11, 381-384.
7. Nguyen, P., & Kim, J.-M. (2016). Adaptive ECG denoising using genetic algorithm based thresholding and ensemble empirical mode decomposition. Information Sciences, 373, 499–511.

8. Qiu, L., Cai, W., Yu, J., Li, W., Chen, Y., Jun, Z., & Wang, Y. (2020). A two-stage ECG signal denoising method based on deep convolutional network. bioRxiv. https://doi.org/10.1101/2020.03.27.012831.

9. Schubert, M. & Schanze, T. (2019). Estimation of sparse VAR models with artificial neural networks for the analysis of biosignals. 2019 41st Annual International Conference of the IEEE Engineering in Medicine and Biology Society (EMBC), Berlin, Germany, 4623-4627. https://10.1109/EMBC.2019.8857403.

10. Samann, F., & Schanze, T. (2021). On estimating the optimal autoencoder model for denoising ECG using Akaike information criterion. AUTOMED -Automation in Medical Engineering2021. zenodo. https://doi.org/10.5281/zenodo.4925814

11. Samann, F., & Schanze, T. (2023). Multiple ECG segments denoising autoencoder model. Biomedical Engineering/ Biomedizinische Technik, 68(3), 1-10. https://doi.org/10.1515/bmt-2022-0199.

12. Samann, F., Meyer, L., & Schanze, T. (2023). Removing noise and overlapping spikes from extracellular recordings using a regularized denoising autoencoder. Accepted: Current Directions in Biomedical Engineering.

13. Sološenko, A., Petrėnas , A., Paliakaitė, B., Marozas, V., & Sörnmo, L. (2021). Model for simulating ECG and PPG signals with arrhythmia episodes. PhysioNet, 101(23).

14. Teoh, E., Tan , K., & Xiang , C. (2006). Estimating the number of hidden neurons singular value decomposition. IEEE Transaction on Neural Networks, 17(6), 1623–1629.

15. Wang, K., Liu, K., Peng, S., & Tsao, Y. (2023). ECG artifact removal from single-channel surface EMG using fully convolutional networks, ICASSP 2023- 2023 IEEE International Conference on Acoustics, Speech and Signal Processing (ICASSP), Rhodes Island, Greece. https://10.1109/ICASSP49357.2023.10096409.

16. Zezario, R., Hussain, T., Zezario, R., Lu, X., Wang, H., & Tsao, Y. (2020). Self-Supervised denoising autoencoder with linear regression decoder for speech Enhancement. 2020 IEEE International Conference on Acoustics, Speech and Signal Processing (ICASSP), 6669–6673.